13C-MFA Delineates the Photomixotrophic Metabolism of Synechocystis sp. PCC 6803 under Light and Carbon Sufficient Conditions

ARTICLE *in* BIOTECHNOLOGY JOURNAL · MAY 2014

Impact Factor: 3.49 · DOI: 10.1002/biot.201300477

5 AUTHORS, INCLUDING:

Le You
University of California, San Diego
17 PUBLICATIONS **112** CITATIONS
SEE PROFILE

Lian He
Washington University in St. Louis
11 PUBLICATIONS **75** CITATIONS
SEE PROFILE

Yinjie Tang
Washington University in St. Louis
83 PUBLICATIONS **1,559** CITATIONS
SEE PROFILE

Biotechnology Journal
www.biotechnology-journal.com

Biotechnol. J. 2014, 9, 684–692

DOI 10.1002/biot.201300477

Research Article

^{13}C-MFA delineates the photomixotrophic metabolism of *Synechocystis* sp. PCC 6803 under light- and carbon-sufficient conditions

Le You[1,*], *Bert Berla*[1,*], *Lian He*[1,*], *Himadri B. Pakrasi*[1,2] *and Yinjie J. Tang*[1]

[1] Department of Energy, Enviromental and Chemical Engineering, Washington University, St. Louis, MO, USA
[2] Department of Biology, Washington University, St. Louis, MO, USA

The central carbon metabolism of cyanobacteria is under debate. For over 50 years, the lack of α-ketoglutarate dehydrogenase has led to the belief that cyanobacteria have an incomplete TCA cycle. Recent in vitro enzymatic experiments suggest that this cycle may in fact be closed. The current study employed ^{13}C isotopomers to delineate pathways in the cyanobacterium *Synechocystis* sp. PCC 6803. By tracing the incorporation of supplemented glutamate into the downstream metabolites in the TCA cycle, we observed a direct in vivo transformation of α-ketoglutarate to succinate. Additionally, isotopic tracing of glyoxylate did not show a functional glyoxylate shunt and glyoxylate was used for glycine synthesis. The photomixotrophic carbon metabolism was then profiled with ^{13}C-MFA under light and carbon-sufficient conditions. We observed that: (i) the in vivo flux through the TCA cycle reactions (α-ketoglutarate → succinate) was minimal (<2%); (ii) the flux ratio of CO_2 fixation was six times higher than that of glucose utilization; (iii) the relative flux through the oxidative pentose phosphate pathway was low (<2%); (iv) high flux through malic enzyme served as a main route for pyruvate synthesis. Our results improve the understanding of the versatile metabolism in cyanobacteria and shed light on their application for photo-biorefineries.

Received	06 NOV 2013
Revised	08 FEB 2014
Accepted	19 MAR 2014
Accepted article online	21 MAR 2014

Supporting information available online

Keywords: Free metabolites · Glyoxylate shunt · Malic enzyme · Pentose phosphate pathway · TCA cycle

Correspondence: Dr. Yinjie J. Tang, Department of Energy, Enviromental and Chemical Engineering, Washington University, St. Louis, MO, 63130, USA
E-mail: yinjie.tang@seas.wustl.edu

Abbreviations: **^{13}C-MFA**, ^{13}C-metabolic flux analysis; **3PG**, 3-phosphoglycerate; **AKG**, α-ketoglutarate; **ALA**, alanine; **ASP**, aspartate; **CIT**, citrate; **DHAP**, dihydroxyacetone phosphate; **E4P**, erythrose 4-phosphate; **F6P**, Fructose 6-phosphate; **FBA**, flux balance analysis; **FUM**, fumarate; **G6P**, glucose 6-phosphate; **GAP**, glyceraldehyde 3-phosphate; **GC–MS**, gas chromatography–mass spectrometry; **GLU**, glutamate; **GLX**, glyoxylate; **GLY**, glycine; **HIS**, histidine; **ICT**, isocitrate; **ILE**, isoleucine; **LEU**, leucine; **MAL**, malate; **MTHF**, 5,10-Methylenetetrahydrofolate; **OAA**, oxaloacetate; **OPP** pathway, oxidative pentose phosphate pathway; **PEP**, phosphoenolpyruvate; **PYR**, pyruvate; **R5P**, ribose 5-phosphate; **Ru5P**, ribulose-5-phosphate; **RuBP**, ribulose-1,5-diphosphate; **S7P**, sedoheptulose-7-phosphate; **SER**, serine; **SUC**, succinate; **TBDMS**, *N-tert*-butyldimethylsilyl-*N*-methyltrifluoroacetamide; **TCA cycle**, tricarboxylic acid cycle; **TMS**: trimethylsilyl; **X5P**, xylulose-5-phosphate.

1 Introduction

Synechocystis sp. PCC 6803 (hereafter *Synechocystis* 6803) is a naturally transformable cyanobacterium [1] and a model organism for studying photosynthesis [2]. *Synechocystis* 6803 and other cyanobacterial species are promising phototrophic cell factories for synthesis of valuable chemicals and biofuels [3–7]. To explore cyanobacterial metabolism for biotechnology applications, genomics and transcriptomics approaches have been used to study *Synechocystis* 6803 [8]. Complementing these approaches, fluxomics tools (flux balance analysis (FBA) and ^{13}C-metabolic flux analysis (^{13}C-MFA)) are also powerful in deciphering genome functions and unraveling cell phenotype in phototrophs under photoautotrophic, pho-

* These authors contributed equally to this work.

tomixotrophic, and heterotrophic metabolisms [9–19]. These multi-omics studies have improved our understanding and application of photo-biorefineries [20].

Nevertheless, cyanobacterial metabolism is still not completely resolved. Due to the lack of α-ketoglutarate dehydrogenase, cyanobacteria were thought to have an incomplete tricarboxylic acid (TCA) cycle [21, 22]. This assumption has been employed in most cyanobacterial models so far [11, 16, 17]. Recently, a pair of enzymes from *Synechococcus* sp. PCC 7002, α-ketoglutarate decarboxylase and succinic semialdehyde dehydrogenase, were found to transform α-ketoglutarate into succinate in vitro [23]. These two enzymes have homologues throughout cyanobacteria. Contemporaneously, Nogales et al. [18] identified an overlapping GABA (γ-aminobutyric acid) shunt in silico that could also complete the TCA cycle via GABA and succinic semialdehyde. Such a pathway in cyanobacteria would help explain previous observations that α-ketoglutarate added to cultures of a *Synechocystis* double mutant strain (knockout of succinate dehydrogenase and fumarate reductase) led to accumulation of succinate [24]. However, an in vivo flux from α-ketoglutarate to succinate has not been measured.

Another open question has been whether the glyoxylate shunt was active or even existed. Glyoxylate shunt activity in some cyanobacterial species were reported [25, 26] and thus were included in the metabolic models of *Synechocystis* 6803 [11, 17, 27, 28]. But homologues encoding isocitrate lyase and malate synthase have still not been found. Moreover, the oxidative pentose phosphate pathway (OPP pathway) in *Synechocystis* 6803 has been considered inactive under light conditions [17], but this pathway was recently proved to be highly active in photoautotrophic metabolism [16].

Considering all these controversial conclusions, we were intrigued to re-delineate the photomixotrophic metabolism in *Synechocystis* 6803. Since the previous application of ^{13}C-MFA to photomixotrophic metabolism was operated in a *Synechocystis* 6803 culture lacking carbonate and atmospheric CO_2 (i.e. CO_2-limiting condition) [17], we were motivated to unravel the central metabolism and reconstruct the metabolic network in *Synechocystis* 6803 under CO_2-sufficient condtions. In addition, the application of ^{13}C-MFA requires the attainment of a metabolic steady state. However, in a photobioreactor, cyanobacteria are continuously moving between "light" (near surface of bioreactor) and "dark" (depending on mixing, cell density, and reactor size/geometry) zones. In the light zone, cells fix CO_2 and accumulate glycogen, while they may use this storage component (or glucose in the medium) for "heterotrophic" metabolism in the dark zone. To minimize such heterogeneous growth, this study has performed ^{13}C-MFA experiments using small culture volume (<50 mL) and low biomass density (OD_{730}<0.5) to ensure cell metabolism under light and carbon-sufficient conditions. This approach may provide a better understanding of photomixotrophic metabolism in *Synechocystis* 6803.

2 Materials and methods

2.1 Photomixotrophic culture

Synechocystis 6803 cultures were grown in a modified BG-11 medium containing no sources of ^{12}C. Ferric ammonium citrate was replaced with ferric ammonium sulfate [29]. ^{13}C was supplied as ~2 g/L $NaH^{13}CO_3$ and 5 g/L glucose (U-$^{13}C_6$ or 1-$^{13}C_1$). The purity of ^{13}C-substrates was >98% (Cambridge Isotope Laboratories, Tewksbury, MA, USA). Inocula from an unlabeled *Synechocystis* 6803 photoautotrophic culture (OD_{730} = ~0.9) was added into 30 mL ^{13}C-labeled medium in 100 mL serum bottles, which were then sealed with rubber septa to prevent atmospheric CO_2 intrusion.

All cultures were started with only a 0.5% inoculation volume to minimize the inoculation effect. Cell growth was under continuous illumination (~50 μmol photons /m^2/s) on a shaker at 150 rpm at 30°C. Cell density was monitored by a UV–Vis spectrophotometer (GENESYS, Thermo Scientific) at 730 nm. The conversion ratio between OD_{730} and dry biomass weight was 1 unit OD_{730} = 0.45 g dry cell weight/L. Total organic carbon analyzer (inorganic carbon measurement mode) with non-dispersive infrared detector (Shimadzu Corporation, Japan) was used to determine sodium bicarbonate concentration in the culture supernatant. Enzyme kits (R-Biopharm, Darmstadt, Germany) were used to measure the glucose concentrations in the culture.

2.2 Isotopic dilution experiments

Isotopic dilution experiments were employed to identify the presence of certain pathways in vivo. To investigate the structure of the TCA cycle, we used glutamate (instead of α-ketoglutarate) as the tracer since cyanobacteria exhibited very low capability to uptake α-ketoglutarate [30]. To examine the presence of the glyoxylate shunt, we used glyoxylate as the tracer. Specifically, unlabeled glutamate (10 mM) or unlabeled glyoxylate (15 mM) was added into ^{13}C-labeled cultures (grown on $NaH^{13}CO_3$ and U-$^{13}C_6$ glucose) during the exponential growth phase (OD_{730} = ~0.4). After 30 min of incubation with a respective tracer, samples from two biological replicates were harvested and free metabolites were extracted. To identify whether *Synechocystis* 6803 used glutamate or glyoxylate for biomass synthesis, *Synechocystis* 6803 cultures were grown with a respective unlabeled tracer (10 mM glutamate or 15 mM glyoxylate), $NaH^{13}CO_3$ and U-$^{13}C_6$ glucose for 48 h (OD_{730} reached ~0.4). Samples from two biological replicates were then collected to analyze the ^{12}C incorporation into proteinogenic amino acids.

2.3 Metabolite extraction and GC-MS analysis

Isotopomer measurements of free metabolites (TMS-based method) and proteinogenic amino acids (TBDMS-based method) are based on previous reports [31–33]. GC-MS analysis had three technical replicates per biological sample.

Intracellular free metabolites were used to qualitatively characterize functional pathways. Supporting information, Fig. S1A–C illustrate the molecular structure of TMS-derivatized amino acids, succinate, and α-ketoglutarate used for analysis. The fragment $[M-15]^+$, minus a methyl group from the TMS group, includes the labeling information of the entire molecule. The $[M-15]^+$ fragment, together with $[M-43]^+$ or $[M-117]^+$(minus the α-carboxyl group from a metabolite), was used for GC–MS analysis.

Proteinogenic amino acids were used to determine the function and quantify the metabolic fluxes. The mass fragments of ten key amino acids provided sufficient constraints for flux calculations [34–36]. The fragments ($[M-57]^+$, $[M-159]^+$ or $[M-85]^+$, and f302) were used for flux analysis [37]. In addition, because of overlap peaks and product degradations, several amino acids (proline, arginine, cysteine, and tryptophan) were not analyzed. The isotopic labeling data are shown as mass fractions, i.e. M0, M1, M2, etc., representing fragments containing unlabeled, singly labeled, and doubly labeled metabolites.

2.4 ^{13}C-metabolic flux analysis

^{13}C-MFA was used to quantify in vivo fluxes through the central metabolic network in *Synechocystis* 6803. Photomixotrophic cultures were grown on 1-$^{13}C_1$ glucose and $NaH^{13}CO_3$. Biomass was collected during the exponential growth phase for proteinogenic amino acids analysis. The metabolic network of *Synechocystis* 6803 was reconstructed based on tracer experiments and previous reports [16, 38–41] that included glycolysis, the Calvin cycle, complete TCA cycle, glyoxylate shunt, and photorespiration pathways (Supporting information, Table S1). In our ^{13}C-MFA, relative metabolic fluxes through the central metabolism were profiled with the assumption that the Calvin cycle flux from Ru5P to RuBP was 100. The minimization of a quadratic function that calculated the difference between predicted and measured isotopomer patterns solved the relative metabolic fluxes (Supporting information, Table S2). The biomass composition (Supporting information, Table S1) was based on a previous report [9]. Reaction reversibility was characterized by the exchange coefficient exch, defined as $v^{exch} = \beta(exch/1-exch)$, where v^{exch} was the exchange flux and β was the exchange constant [42]. In this study, β was equal to 500 and exch ranged from 0 to 1. The forward flux ($v^{forward}$) and backward flux ($v^{backward}$) in the model were transformed from the v^{exch} and the net flux, v^{net}, using following equation [43]:

$$\begin{pmatrix} v\mathbf{forward} \\ v\mathbf{backward} \end{pmatrix} = \begin{pmatrix} v\mathbf{exch} - \mathbf{min}(-v\mathbf{net}, 0) \\ v\mathbf{exch} - \mathbf{min}(v\mathbf{net}, 0) \end{pmatrix}.$$

The optimization for ^{13}C-MFA was performed as follows:

$$\min (\mathbf{M_{exp}} - \mathbf{M_{sim}(v)})^{\mathbf{T}} (\mathbf{M_{exp}} - \mathbf{M_{sim}(v)}) \quad (1)$$

$$\text{s.t.}\ \mathbf{v} \in \mathbf{(lb, ub)} \quad (2)$$

$$\mathbf{S} \cdot \mathbf{v} = \mathbf{0}, \quad (3)$$

$$\mathbf{A_i} \cdot \mathbf{X_i} = \mathbf{B_i} \cdot \mathbf{Y_i}\ (i=1, 2, 3, 4, 5) \quad (4)$$

Equation 1 is the quadratic error function that was optimized and M_{exp} is the vector of experimentally measured labeling patterns of amino acids. M_{sim} is the counterpart of the simulated data as a function of fluxes. v is the flux vector that is to be determined. Equation 2 gives the boundary conditions of the flux variables. Equation 3 represents the metabolite balances. Equation 4 represents the elementary metabolite unit (EMU) balance, where X_i and Y_i represent the unknown and known EMU variables of size i, respectively, and A_i and B_i are matrices of linear functions of the fluxes [44, 45].

The MATLAB optimization solver "fmincon" was employed to minimize the quadratic error function. To avoid local minima, 100 initial guesses were randomly generated, and the solution set that minimized the objective function was used as the best fit. The Monte Carlo method was used to calculate 95% confidence intervals [46]. The measured isotopomer data was perturbed 1000 times with normally distributed noise within measurement error, and the optimization solver was restarted with the optimal solution. The determination of confidence intervals of the fluxes (95%) was based on 1000 simulations, and confidence intervals were used to calculate standard deviations.

3 Results

3.1 Photomixotrophic biomass growth and metabolic pseudo-steady state

Figure 1 shows the growth curves in serum bottles and shake flasks. Cell doubling times were similar in both containers. The similarity of growth indicates that O_2 accumulation in the serum bottle headspace had minimal effect on photomixotrophic growth. During the early growth phase, the specific growth rate in the early exponential phase was 0.079/h. After cultivation in serum bottles for 75 h, cell growth slowed down and the culture pH rose from 8 to 10.

To determine a pseudo-steady state metabolic period for ^{13}C-MFA, biomass samples from serum bottles were

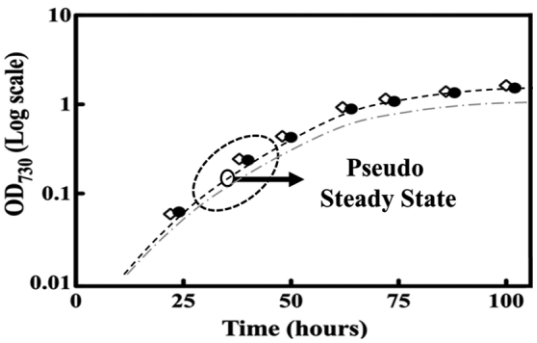

Figure 1. Growth curve of *Synechocystis* 6803 under photomixotrophic conditions. The cultures were grown in shake flasks (open circles) or serum bottles (closed circles) in modified liquid BG-11 medium supplemented with 5 g/L glucose and ~2 g/L sodium bicarbonate. The circle highlights the metabolic pseudo-steady state period of cultivation. The dot-dash line represents the growth curve under photoautotrophic conditions (in shake flasks). Each symbol represents the mean value of biological triplicate cultures.

collected at different time points to analyze amino acid labeling (Supporting information, Table S2). The labeling patterns in biomass protein were relatively stable (standard deviation were below 0.01) between samples taken within the first 48-h cultures (Supporting information, Table S2). Thereby, our ^{13}C-MFA was based on ^{13}C-biomass samples taken at early growth phase (OD_{730} = ~0.4, Supporting information, Table S2).

3.2 ^{13}C-based pathway investigation

Based on isotopic dilution of downstream metabolites after incubating cell with unlabeled precursors, in vivo enzyme functions were investigated in tracer experiments. Prior to ^{12}C-glutamate pulse treatment, α-ketoglutarate (Fig. 2A), succinate (Fig. 2B), and malate (Fig. 2C) were nearly fully labeled (M5 for α-ketoglutarate; M4 for succinate and malate) in ^{13}C labeled cultures. After 30-min incubation with unlabeled glutamate, ^{12}C carbon from glutamate was incorporated into the downstream metabolites of α-ketoglutarate. ^{12}C abundance increased to over 65% in succinate, 90% in α-ketoglutarate, and 30% in malate. Mass spectra of these metabolites before and after glutamate addition are shown in Supporting information, Fig. S1. After incubation with unlabeled glutamate for 48 h, all amino acids, except glutamate, from biomass protein remained fully ^{13}C labeled (Fig. 3 and Supporting information Fig. S2).

Labeled cultures pulsed with unlabeled glyoxylate showed a shift from fully ^{13}C to ^{12}C in free glycine and glyoxylate (M2 to M0, Fig. 4A). However, no significant shift was observed in succinate and α-ketoglutarate, both of which are downstream metabolites of malate. After the labeled culture was incubated with unlabeled glyoxylate for 48 h, ^{12}C was only incorporated into proteinogenic glycine (Fig. 4B), while other proteinogenic amino acids remained highly labeled.

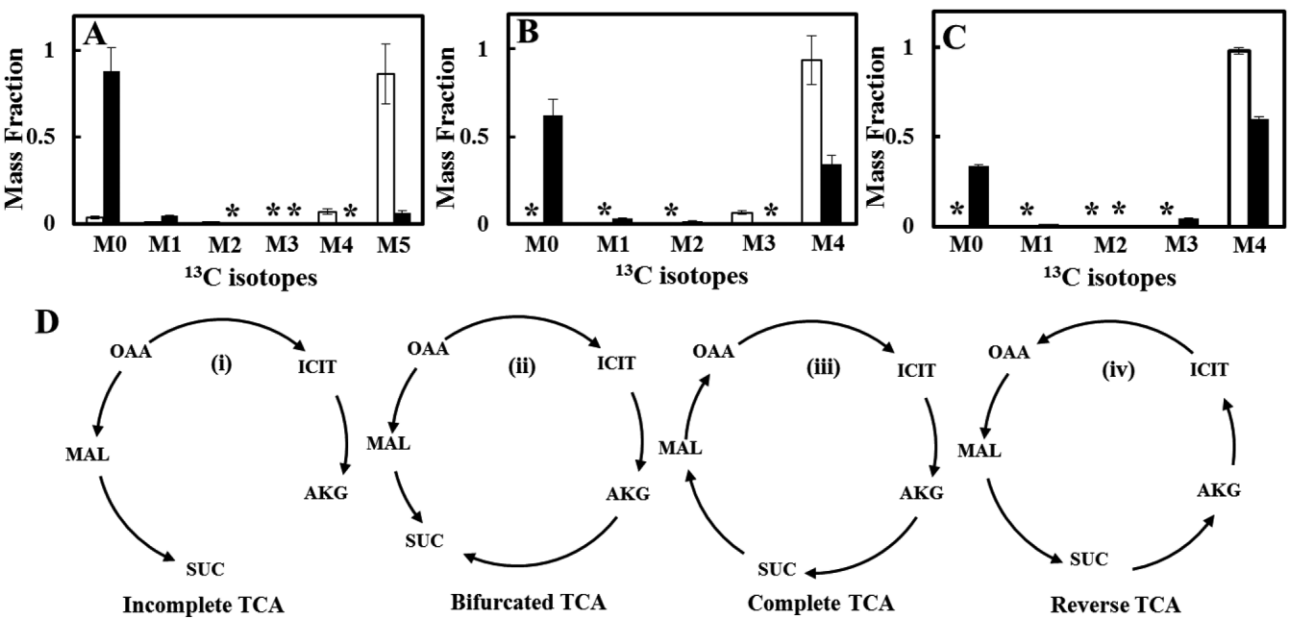

Figure 2. Tracing the *Synechocystis* TCA pathway by isotopic dilution experiments. (**A**–**C**) show the isotopomer distributions of the $[M-15]^+$ fragment in α-ketoglutarate, succinate, and malate (data from biological duplicates and technical triplicates). *Synechocystis* 6803 was grown in the labeled medium with U-^{13}C glucose and $NaH^{13}CO_3$. Unlabeled glutamate was added during OD_{730} = ~0.4. Biomass samples were harvested after 30-min incubation from cultures with (■) or without (□) unlabeled glutamate. Error bars indicate standard deviations of averages from two biological and three technical replicates. Stars in the figures indicate 0 values. (**D**) shows different scenarios of microbial TCA pathways.
Abbreviation: AKG, α-ketoglutarate; ICT, isocitrate; MAL, malate; OAA, oxaloacetate; SUC, succinate.

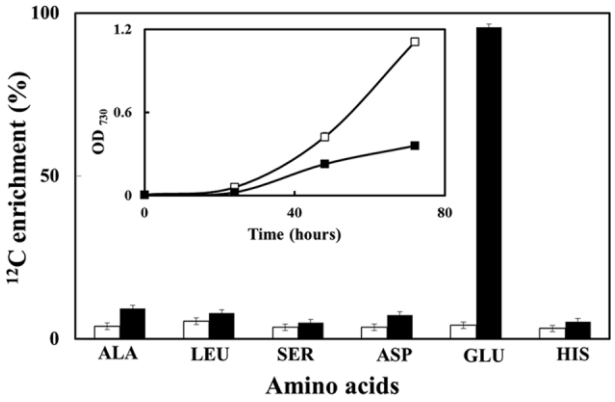

Figure 3. Long-term tracer experiment results with unlabeled glutamate. Biomass samples (OD_{730} = ~0.4, data from biological duplicates and technical triplicates) were harvested after a 48-h incubation in fully labeled photomixotrophic cultures with (■) or without (□) unlabeled glutamate. The ^{12}C-enrichment is calculated by (*n* is the total carbon number of an amino acid; *M* the relative molar concentration of mass isotopomer *n* – *i*). The error bars in the figure represent the standard deviation among samples (*n* = 2). The inset figure shows growth of cultures with (■) or without (□) unlabeled glutamate (i.e. glutamate inhibited growth).
Abbreviation: ALA, alanine; ASP, aspartate; GLU, glutamate; HIS, histidine; LEU, leucine; SER, serine.

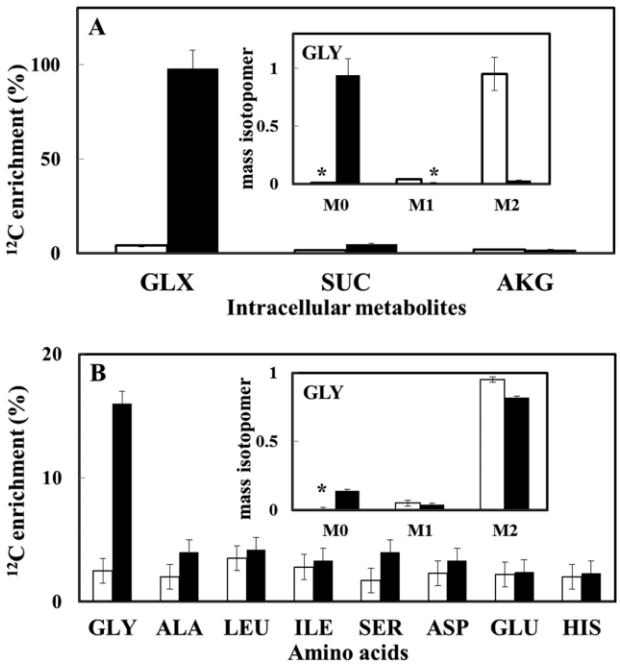

Figure 4. Tracing the *Synechocystis* glyoxylate shunt. (**A**) shows the ^{12}C-ratio of free metabolites. Biomass samples were harvested after 30-min incubation in fully labeled cultures (OD_{730} = ~0.4) with (■) or without (□) unlabeled glyoxylate. The inset shows the isotopomer distribution of free glycine. (**B**) shows the ^{12}C-enrichment of proteinogenic amino acids (*n* = 2). Biomass samples were harvested after a 48-h incubation in fully labeled cultures with (■) or without (□) unlabeled glyoxylate. The inset shows the isotopomer distribution of proteinogenic glycine. The error bars represent the standard deviations of averages from two biological and three technical replicates. Stars in the figure indicate that the MS peaks cannot be detected by GC–MS.
Abbreviation: AKG, α-ketoglutarate; ALA, alanine; ASP, aspartate; GLU, glutamate; GLX, glyoxylate; GLY, glycine; HIS, histidine; ICT, isocitrate; ILE, isoleucine; LEU, leucine; MAL, malate; OAA, oxaloacetate; SER, serine; SUC, succinate.

3.3 Flux analysis results

^{13}C-MFA results are sensitive to model network construction, the labeling patterns of substrates, and the completeness of isotopomer data. In this study, the isotopic dilution experiments were employed to reveal the metabolic network in *Synechocystis* 6803. Singly labeled glucose and fully labeled bicarbonate were used to generate unique isotopomer data in amino acids. Via EMU simulations and isotopomer information from different MS fragments, ^{13}C-MFA profiled the photomixotrophic metabolism under light and carbon-sufficient conditions. Relative flux distributions, exchange coefficients for reversible reactions, and 95% confidence intervals are shown in Fig. 5 and Supporting information, Table S1. The simulated fluxes fit the isotopomer data well (r^2>0.99, Supporting information, Fig. S3).

^{13}C-MFA indicated that *Synechocystis* 6803 had a high CO_2 fixation flux through the Calvin cycle (~100) than the glucose uptake flux (~18) in the early photomixotrophic growth phase. Consistent with this observation, <0.1 g/L glucose was consumed during early growth phase. In contrast, previous ^{13}C-MFA of photomixotrophic metabolism in *Synechocystis* 6803 under CO_2 limiting conditions found the glucose uptake flux to be ~50 [17]. In another study, when cell culture was dense (OD_{730} up to 20), *Synechocystis* 6803 utilized significantly more glucose than CO_2 for its growth [47]. Thereby, CO_2 and light conditions can significantly affect the photomixotrophic metabolism in *Synechocystis* 6803.

Under photomixotrophic conditions with sufficient light and carbon sources, the flux from α-ketoglutarate to succinate was not significant (<2% of total CO_2 uptake). Most of the flux from α-ketoglutarate went to glutamate biosynthesis. The glyoxylate shunt did not show a measureable flux (<0.1% of total CO_2 uptake). Additionally, the OPP pathway showed a measurable flux (1.9% of total CO_2 uptake), which played a minor role in C5 carbon synthesis and NADPH production. The flux through photorespiration, however, was limited to 0.1% of total CO_2 uptake. Although the confidence intervals (Supporting information, Table S1) of these anaplerotic reactions (PEP + CO_2 → OAA; MAL → CO_2 + PYR) were larger than those of other fluxes, malic enzyme still showed significant flux and was the main route for pyruvate synthesis.

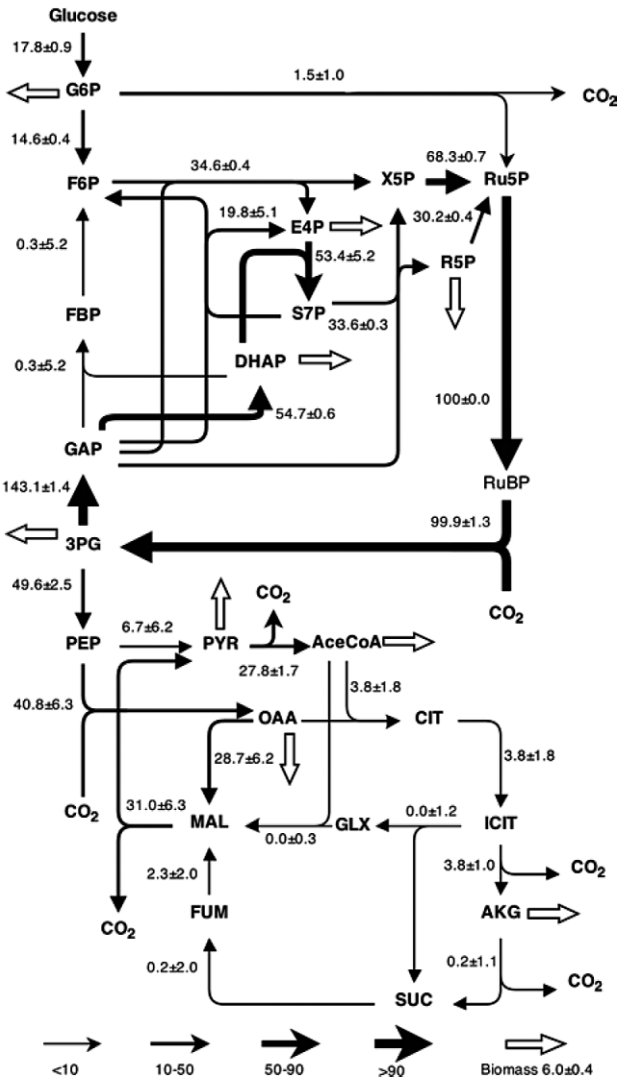

Figure 5. Flux distribution in the central metabolism of *Synechocystis* 6803 under photomixotrophic conditions. All the estimated relative flux rates are shown beside the pathways, which are normalized to the Calvin cycle flux (note: Ru5P → RuBP flux was assumed to be 100). The standard deviation of each flux is shown, which was calculated based on the 95% confidence intervals (Supporting information, Table S1). The white arrows represent the fluxes to biomass. The estimated glucose consumption rate was 0.24 mmol (g dry cell weight)$^{-1}$ h^{-1} (Supporting information S2). FUM was also a byproduct of biomass synthesis (Supporting information, Table S1).

Abbreviation: 3PG, 3-phosphoglycerate; AKG, α-ketoglutarate; ALA, alanine; ASP, aspartate; CIT, citrate; DHAP, dihydroxyacetone phosphate; E4P, erythrose 4-phosphate; F6P, Fructose 6-phosphate; FUM, fumarate; G6P, glucose 6-phosphate; GAP, glyceraldehyde 3-phosphate; GLU, glutamate; GLX, glyoxylate; GLY, glycine; HIS, histidine; ICT, isocitrate; ILE, isoleucine; LEU, leucine; MAL, malate; MTHF, 5,10-methylenetetrahydrofolate; OAA, oxaloacetate; PEP, phosphoenolpyruvate; PYR, pyruvate; R5P, Ribose 5-phosphate; Ru5P, ribulose-5-phosphate; RuBP, ribulose-1,5-diphosphate; S7P, sedoheptulose-7-phosphate; SER, serine; SUC, succinate; THF, tetrahydrofolate; X5P, xylulose-5-phosphate.

4 Discussion

4.1 TCA cycle metabolism

Cyanobacteria are prokaryotes responsible for the conversion of the early atmosphere into our current oxygen-rich atmosphere [48]. Primitive anaerobic prokaryotes developed two separate TCA pathways: the reductive branch (oxaloacetate to succinate) and the oxidative branch (citrate to α-ketoglutarate) (Fig. 2D(i)). Some anaerobic bacteria, such as *Clostridium acetobutylicum*, use a bifurcated TCA cycle that terminates at succinate (Fig. 2D(ii)). As atmospheric oxygen levels rose, the two branches linked to complete the TCA cycle. For example, the TCA cycle in facultative anaerobes (e.g. *E. coli*) can be complete if oxygen is present (Fig. 2D(iii)). A phototrophic bacterium, *Chlorobaculum tepidum,* employs a reverse TCA cycle [49] (Fig. 2D(iv)).

In our study, the labeling patterns of free metabolites indicated that the pathway for converting α-ketoglutarate to succinate can be complete under glutamate addition conditions. Significant amounts of unlabeled α-ketoglutarate, succinate, and malate (Fig. 2A–C) were observed after unlabeled glutamate was added into ^{13}C labeled cultures. Since α-ketoglutarate dehydrogenase activity has never been shown to exist in cyanobacteria, we presume that this conversion was accomplished by a newly discovered pathway through succinic semialdehyde [10, 18, 23]. On the other hand, key proteinogenic amino acids, e.g. aspartate (derived from oxaloacetate), alanine (derived from pyruvate), and serine (derived from 3-phosphoglycerate), had very little ^{12}C incorporation (<5%) from glutamate after 2-day incubation with unlabeled glutamate (Fig. 3). These results qualitatively indicated that the flux from α-ketoglutarate towards the complete TCA cycle was very small compared to other fluxes (e.g. fluxes through glycolysis and the Calvin cycle). The low conversion from α-ketoglutarate to its TCA cycle downstream metabolites was also observed in a *Synechococcus elongatus* PCC 7942 mutant (with an engineered α-ketoglutarate permease), in which α-ketoglutarate was mainly converted into glutamate and glutamine instead of TCA cycle downstream metabolites [30].

Although our ^{13}C-study cannot distinguish whether the conversion of α-ketoglutarate to succinate was via α-ketoglutarate decarboxylase or the GABA shunt [18], this reaction may be notable in cyanobacterial metabolism only under certain conditions (e.g. with the presence of large amount of glutamate or α-ketoglutarate). The poor activity of this reaction may also explain why the previous tracer studies did not observe the conversion of α-ketoglutarate to succinate. These studies used an assay of α-ketoglutarate dehydrogenase activity [21], as opposed to the decarboxylase activity that has been more recently observed to convert α-ketoglutarate to succinate [23].

Although many cyanobacterial species appear to have a complete TCA cycle pathway, it may not be adapted to carry a large flux. A recent FBA model indicates that a complete cyanobacterial TCA cycle via AKG dehydrogenase may reduce biomass growth due to the unnecessary metabolic burden for the synthesis of multi-protein enzymes [19]. For organisms that obtain sufficient reducing equivalents from light reactions, the use of a complete TCA cycle to oxidize carbon is unnecessary. Thereby, the complete TCA pathways in *Synechocystis* 6803 may serve only to regenerate intermediates or fine-tune the metabolic balance under certain photomixotrophic conditions (such as the presence of extracellular glutamate).

4.2 The glyoxylate shunt

This study also examined the presence of the glyoxylate shunt and determined its function in *Synechocystis* 6803. Previous metabolic models predicted that *Synechocystis* 6803 contains a bacterial-like glyoxylate shunt [17]. However, *Synechocystis* 6803, and nearly all other sequenced cyanobacteria, lack homologues of known genes that encode isocitrate lyase and malate synthase. Some ^{13}C-MFA [16] and FBA [11, 15] studies have also suggested that the glyoxylate shunt in *Synechocystis* 6803 was incomplete under photoautotrophic and photomixotrophic conditions. In our tracer experiments with the addition of unlabeled glyoxylate during the exponential phase, we observed the uptake of glyoxylate and its conversion to glycine (Fig. 4A). However, in the proteinogenic amino acids of ^{13}C-cultures grown with ^{12}C glyoxylate (Fig. 4B), we did not see significant ^{12}C accumulation in proteinogenic amino acids downstream of malate (i.e. the end-product of the glyoxylate shunt), including alanine and aspartate (Fig. 4B). Statistically, ^{13}C-MFA showed that the in vivo flux through the presumed glyoxylate shunt was essentially zero (Fig. 5). This observation of the glyoxylate shunt is supported by a recent enzymatic test using crude extracts of *Synechocystis* 6803 cells, in which no isocitrate lyase activity was detected [19].

4.3 Malic enzyme activity

Under continuous light illumination, the malic enzyme is important for optimal *Synechocystis* 6803 growth. This gene (*slr0721*) is highly expressed under photomixotrophic conditions compared to photoautotrophic conditions [8]. Moreover, ^{13}C-MFA revealed significant malic enzyme flux in *Synechocystis* 6803 under photoautotrophic [16] and CO_2 limited photomixotrophic cultures [17]. Previous reports indicated that the malic enzyme reaction (malate $\rightarrow$ pyruvate + CO_2 + NADPH) is instrumental in a carbon concentrating mechanism akin to that in C4 plants, and this enzyme may indirectly transport NADPH between different cell locations. In this study, high malic enzyme activity was also observed when the bicarbonate and reduced carbon source were sufficient. In fact, deletion of malic enzyme gene significantly reduces *Synechocystis* 6803 growth under both photoautotrophic and glucose-based photomixotrophic conditions, while the growth can be recovered by providing pyruvate [50]. Thereby, high flux through malic enzyme (~31) is likely to serve as a key route for pyruvate synthesis when pyruvate kinase is inhibited by ATP, a negative allosteric inhibitor under photosynthetic conditions [50].

4.4 The oxidative pentose phosphate pathway

The OPP pathway is an important NADPH synthesis route in heterotrophic organisms. Since photosynthetic light reactions produce significant amounts of NADPH, the OPP pathway becomes futile in phototrophic metabolism. A cyanobacterial mutant (Δ*zwf*) of *Synechococcus* sp. strain PCC 7942, that lacks the OPP pathway enzymes, exhibited a similar growth rate to the wild-type strain under photoautotrophic conditions [51]. Moreover, glucose in phototrophic cultures has been shown to either increase or have a small effect on key OPP pathway enzyme transcriptions [8, 52, 53]. Taken together, these data indicate that the OPP pathway is dispensable under light conditions. On the other hand, the OPP pathway mutant described above exhibited decreased viability under dark incubations [51]. FBA models also predicted that the OPP pathway was active under light-limited conditions [11]. Our experiments measured a low flux (~1.5) through the OPP pathway under early photomixotrophic growth conditions (i.e. light- and carbon-sufficient culture). However, during the late growth phase (Supporting information, Table S2), the biomass showed a higher unlabeled proteinogenic histidine (M0 fraction, Supporting information, Table S2), indicating that more glucose was directed to OPP for ribose-5-phosphate synthesis (precursor of histidine). These results suggested a flexibility of the OPP pathway in balancing NADPH under different light and carbon conditions.

4.5 Limitations of our ^{13}C-MFA techniques for cyanobacterial study

There are several limitations in ^{13}C-MFA techniques for cyanobacterial study. First, ^{13}C-MFA accuracy is highly dependent on metabolic model constructions. Nevertheless, incomplete annotations, errors, or inconsistencies are prevalent in cyanobacterial genome databases, rendering it difficult to generate a comprehensive metabolic network for ^{13}C-MFA. Tracer experiments were used here to examine the structure of cyanobacterial metabolic network. Since the key intemediate tracers (e.g. ^{13}C-glutamate and ^{13}C-glyoxylate) are prohibitively expensive, an inverse tracer labeling approach was employed to save experimental costs. A ^{13}C-culture background was first built with commonly used ^{13}C-substrates (bicarbonate

and glucose). Unlabeled glutamate or glyoxylate were then added into the ^{13}C-cultures as tracers. Their incorporation into downstream metabolites were used to determine pathway functions. Since the addition of intermediate tracers may change cell metabolism, the results from isotopic dilution experiments were used to validate the metabolic model.

Second, ^{13}C-MFA cannot precisely determine certain pathways. For example, the confidence intervals of anaplerotic fluxes are much larger than those of other fluxes. Additional information, such as genetic analyses, is required to validate flux analysis results.

Third, the application of ^{13}C-MFA requires the attainment of a steady state with minimal labeling changes in the central metabolism. Therefore, metabolisms under photoautotrophic or circadian conditions cannot be analyzed using traditional ^{13}C-MFA. Although an advanced isotopic non-stationary MFA has been developed to capture the transient states of metabolic networks, it is difficult to precisely measure the labeling patterns of low-abundance and unstable free metabolites. It is also difficult to resolve the unexpected labeling kinetics of free metabolites caused by metabolic channeling or light heterogeneity inside of photo-bioreactors [16]. Furthermore, the degradation–regeneration of certain cellular polymers (e.g. cyanophycin) may cause the dynamic exchange of carbons between free metabolites and macromolecules, interfering the non-stationary metabolite labeling [54]. Therefore, this study is only able to profile a steady-state ^{13}C-MFA under mixotrophic conditions.

Finally, *Synechocystis* 6803's metabolism is diverse and affected by both light and carbon conditions, so the observed results in this study pertain solely to photomixotrophic conditions when light and carbon sources are sufficient.

5 Conclusion

This study used ^{13}C-metabolism analysis to delineate the photomixotrophic metabolism of *Synechocystis* 6803. ^{13}C-analysis confirmed the in vivo conversion of α-ketoglutarate to succinate when an additional source was supplied to increase the α-ketoglutarate pool size (e.g. glutamate) while this flux under photomixotrophic conditions is negligible compared to all other fluxes in the model. Glyoxylate was discovered as a potential source for glycine synthesis, while the activity of the glyoxylate shunt was not observed. Under photomixotrophic conditions, malic enzyme, rather than pyruvate kinase, is a fundamental route for pyruvate synthesis. Oxidative pentose phosphate pathway flux is low when light and inorganic carbon is sufficient. These findings complement information of previous multiple-omics studies, which have shown that ^{13}C-tools greatly advance the understanding of cellular metabolisms. This study also suggests that the photomixotrophic metabolism of cyanobacteria can efficiently incorporate both sugar and CO_2 for biosynthesis, resulting in potentially higher biomass density and productivity.

This research was funded by an NSF Career Grant (MCB0954016). It was also supported by the Office of Science (BER), U. S. Department of Energy (DE-SC0006870), and the Consortium for Clean Coal Utilization at Washington University in St. Louis to HBP. We thank James Ballard and Katrina Leyden for their writing assistance.

The authors declare no commercial or financial conflict of interest.

6 References

[1] Grigorieva, G., Shestakov, S., Transformation in the cyanobacterium *Synechocystis* sp. 6803. *FEMS Microbiol. Lett.* 1982, *13*, 367–370.
[2] Berry, S., Schneider, D., Vermaas, W. F., Rögner, M., Electron transport routes in whole cells of *Synechocystis* sp. strain PCC 6803: The role of the cytochrome bd-type oxidase. *Biochemistry* 2002, *41*, 3422–3429.
[3] Atsumi, S., Higashide, W., Liao, J. C., Direct photosynthetic recycling of carbon dioxide to isobutyraldehyde. *Nat. Biotechnol.* 2009, *27*, 1177–1180.
[4] Chisti, Y., Biodiesel from microalgae beats bioethanol. *Trends Biotechnol.* 2008, *26*, 126–131.
[5] Lan, E. I., Liao, J. C., Metabolic engineering of cyanobacteria for 1-butanol production from carbon dioxide. *Metab. Eng.* 2011, *13*, 353–363.
[6] Lindberg, P., Park, S., Melis, A., Engineering a platform for photosynthetic isoprene production in cyanobacteria, using Synechocystis as the model organism. *Metab. Eng.* 2010, *12*, 70–79.
[7] Deng, M.-D., Coleman, J. R., Ethanol synthesis by genetic engineering in cyanobacteria. *Appl. Environ. Microbiol.* 1999, *65*, 523–528.
[8] Yoshikawa, K., Hirasawa, T., Ogawa, K., Hidaka, Y. et al., Integrated transcriptomic and metabolomic analysis of the central metabolism of *Synechocystis* sp. PCC 6803 under different trophic conditions. *Biotechnol. J.* 2013, *8*, 571–580.
[9] Saha, R., Verseput, A. T., Berla, B. M., Mueller, T. J. et al., Reconstruction and comparison of the metabolic potential of cyanobacteria *Cyanothece* sp. ATCC 51142 and *Synechocystis* sp. PCC 6803. *PLoS One* 2012, *7*, e48285.
[10] Knoop, H., Zilliges, Y., Lockau, W., Steuer, R., The metabolic network of *Synechocystis* sp. PCC 6803: Systemic properties of autotrophic growth. *Plant Physiol.* 2010, *154*, 410–422.
[11] Shastri, A. A., Morgan, J. A., Flux balance analysis of photoautotrophic metabolism. *Biotechnol. Progr.* 2005, *21*, 1617–1626.
[12] Yang, C., Hua, Q., Shimizu, K., Quantitative analysis of intracellular metabolic fluxes using GC-MS and two-dimensional NMR spectroscopy. *J. Biosci. Bioeng.* 2002, *93*, 78–87.
[13] McKinlay, J. B., Harwood, C. S., Carbon dioxide fixation as a central redox cofactor recycling mechanism in bacteria. *Proc. Natl Acad. Sci.* 2010, *107*, 11669–11675.
[14] McKinlay, J. B., Harwood, C. S., Calvin cycle flux, pathway constraints, and substrate oxidation state together determine the H_2 biofuel yield in photoheterotrophic bacteria. *MBio* 2011, *2*, e00323-10.

[15] Yoshikawa, K., Kojima, Y., Nakajima, T., Furusawa, C. et al., Reconstruction and verification of a genome-scale metabolic model for *Synechocystis* sp. PCC6803. *Appl. Microbiol. Biotechnol.* 2011, *92*, 347–358.
[16] Young, J. D., Shastri, A. A., Stephanopoulos, G., Morgan, J. A., Mapping photoautotrophic metabolism with isotopically nonstationary ^{13}C flux analysis. *Metab. Eng.* 2011, *13*, 656–665.
[17] Yang, C., Hua, Q., Shimizu, K., Metabolic flux analysis in *Synechocystis* using isotope distribution from ^{13}C-labeled glucose. *Metab. Eng.* 2002, *4*, 202–216.
[18] Nogales, J., Gudmundsson, S., Knight, E. M., Palsson, B. O., Thiele, I., Detailing the optimality of photosynthesis in cyanobacteria through systems biology analysis. *Proc. Natl. Acad. Sci.* 2012, *109*, 2678–2683.
[19] Knoop, H., Gründel, M., Zilliges, Y., Lehmann, R. et al., Flux balance analysis of cyanobacterial metabolism: The metabolic network of *Synechocystis* sp. PCC 6803. *PLoS Comput. Biol.* 2013, *9*, e1003081.
[20] Kohlstedt, M., Becker, J., Wittmann, C., Metabolic fluxes and beyond – systems biology understanding and engineering of microbial metabolism. *Appl. Microbiol. Biotechnol.* 2010, *88*, 1065–1075.
[21] Pearce, J., Leach, C. K., Carr, N. G., The incomplete tricarboxylic acid cycle in the blue-green alga *Anabaena variabilis*. *J. General Microbiol.* 1969, *55*, 371–378.
[22] Smith, A. J., London, J., Stanier, R. Y., Biochemical basis of obligate autotrophy in blue-green algae and thiobacilli. *J. Bacteriol.* 1967, *94*, 972–983.
[23] Zhang, S., Bryant, D. A., The tricarboxylic acid cycle in cyanobacteria. *Science* 2011, *334*, 1551–1553.
[24] Cooley, J. W., Howitt, C. A., Vermaas, W. F. J., Succinate:quinol oxidoreductases in the cyanobacterium *Synechocystis* sp. Strain PCC 6803: Presence and function in metabolism and electron transport. *J. Bacteriol.* 2000, *182*, 714–722.
[25] Eley, J. H., Glyoxylate cycle enzyme activities in the cyanobacterim *Anacystis nidulans*. *J. Phycol.* 1988, *24*, 586–588.
[26] Pearce, J., Carr, N., The metabolism of acetate by the blue-green algae, *Anabaena variabilis* and *Anacystis nidulans*. *J. Gen Microbiol.* 1967, *49*, 301–313.
[27] Montagud, A., Navarro, E., Fernandez de Cordoba, P., Urchueguia, J., Patil, K., Reconstruction and analysis of genome-scale metabolic model of a photosynthetic bacterium. *BMC Syst. Biol.* 2010, *4*, 156.
[28] Fu, P., Genome-scale modeling of *Synechocystis* sp. PCC 6803 and prediction of pathway insertion. *J. Chem. Technol. Biotechnol.* 2009, *84*, 473–483.
[29] Katoh, H., Hagino, N., Ogawa, T., Iron-binding activity of FutA1 subunit of an ABC-type iron transporter in the cyanobacterium *Synechocystis* sp. Strain PCC 6803. *Plant Cell Physiol.* 2001, *42*, 823–827.
[30] Vázquez-Bermúdez, M. F., Herrero, A., Flores, E., Uptake of 2-oxoglutarate in *Synechococcus* strains transformed with the *Escherichia coli kgtP* Gene. *J. Bacteriol.* 2000, *182*, 211–215.
[31] Meadows, A. L., Kong, B., Berdichevsky, M., Roy, S. et al., Metabolic and morphological differences between rapidly proliferating cancerous and normal breast epithelial cells. *Biotechnol. Progr.* 2008, *24*, 334–341.
[32] Tang, Y. J., Shui, W. Q., Myers, S., Feng, X. et al., Central metabolism in *Mycobacterium smegmatis* during the transition from O_2-rich to O_2-poor conditions as studied by isotopomer-assisted metabolite analysis. *Biotechnol. Lett.* 2009, *31*, 1233–1240.
[33] You, L., Page, L., Feng, X., Berla, B. et al., Metabolic pathway confirmation and discovery through ^{13}C-labeling of proteinogenic amino acids. *J. Vis. Exp.* 2012, e3583.
[34] Pingitore, F., Tang, Y. J., Kruppa, G. H., Keasling, J. D., Analysis of amino acid isotopomers using FT-ICR MS. *Anal. Chem.* 2007, *79*, 2483–2490.
[35] Tang, Y. J., Hwang, J. S., Wemmer, D., Keasling, J. D., The *Shewanella oneidensis* MR-1 fluxome under various oxygen conditions. *Appl. Environ. Microbiol.* 2007, *73*, 718–729.
[36] Tang, Y. J., Martin, H. G., Dehal, P. S., Deutschbauer, A. et al., Metabolic flux analysis of *Shewanella* spp. reveals evolutionary robustness in central carbon metabolism. *Biotechnol. Bioeng.* 2009, *102*, 1161–1169.
[37] Antoniewicz, M. R., Kelleher, J. K., Stephanopoulos, G., Accurate assessment of amino acid mass isotopomer distributions for metabolic flux analysis. *Anal. Chem.* 2007, *79*, 7554–7559.
[38] Smith, A. J., Modes of cyanobacterial carbon metabolism. *Annal. l'Inst. Pasteur Microbiol.* 1983, *134*, 93–113.
[39] Bauwe, H., Hagemann, M., Fernie, A. R., Photorespiration: Players, partners and origin. *Trends Plant Sci.* 2010, *15*, 330–336.
[40] Pelroy, R. A., Bassham, J. A., Photosynthetic and dark carbon metabolism in unicellular blue-green algae. *Arch. Mikrobiol.* 1972, *86*, 25–38.
[41] Robert Tabita, F., The biochemistry and molecular regulation of carbon dioxide metabolism in cyanobacteria, in: Bryant, D. (Ed.), *The Molecular Biology of Cyanobacteria*, Springer Netherlands 2004, pp. 437–467.
[42] Dauner, M., Bailey, J. E., Sauer, U., Metabolic flux analysis with a comprehensive isotopomer model in *Bacillus subtilis*. *Biotechnol. Bioeng.* 2001, *76*, 144–156.
[43] Wiechert, W., Siefke, C., de Graaf, A. A., Marx, A., Bidirectional reaction steps in metabolic networks: II. Flux estimation and statistical analysis. *Biotechnol. Bioeng.* 1997, *55*, 118–135.
[44] Antoniewicz, M. R., Kelleher, J. K., Stephanopoulos, G., Elementary metabolite units (EMU): A novel framework for modeling isotopic distributions. *Metab. Eng.* 2007, *9*, 68–86.
[45] Leighty, R. W., Antoniewicz, M. R., Parallel labeling experiments with [U-^{13}C]glucose validate *E. coli* metabolic network model for ^{13}C metabolic flux analysis. *Metab. Eng.* 2012, *14*, 533–541.
[46] Zhao, J., Shimizu, K., Metabolic flux analysis of *Escherichia coli* K12 grown on ^{13}C-labeled acetate and glucose using GC-MS and powerful flux calculation method. *J. Biotechnol.* 2003, *101*, 101–117.
[47] Varman, A. M., Xiao, Y., Pakrasi, H. B., Tang, Y. J., Metabolic Engineering of *Synechocystis* sp. Strain PCC 6803 for Isobutanol Production. *Appl. Environ. Microbiol.* 2013, *79*, 908–914.
[48] Riding, R., Cyanobacterial calcification, carbon dioxide concentrating mechanisms, and Proterozoic–Cambrian changes in atmospheric composition. *Geobiology* 2006, *4*, 299–316.
[49] Feng, X., Tang, K.-H., Blankenship, R. E., Tang, Y. J., Metabolic flux analysis of the mixotrophic metabolisms in the green sulfur bacterium *Chlorobaculum tepidum*. *J. Biol. Chem.* 2010, *285*, 39544–39550.
[50] Bricker, T. M., Zhang, S., Laborde, S. M., Mayer, P. R. et al., The malic enzyme is required for optimal photoautotrophic growth of *Synechocystis* sp. strain PCC 6803 under continuous light but not under a diurnal light regimen. *J. Bacteriol.* 2004, *186*, 8144–8148.
[51] Scanlan, D. J., Sundaram, S., Newman, J., Mann, N. H., Carr, N. G., Characterization of a *zwf* mutant of *Synechococcus* sp. strain PCC 7942. *J. Bacteriol.* 1995, *177*, 2550–2553.
[52] Yang, C. Y., Hua, Q. H., Shimizu, K. S., Integration of the information from gene expression and metabolic fluxes for the analysis of the regulatory mechanisms in *Synechocystis*. *Appl. Microbiol. Biotechnol.* 2002, *58*, 813–822.
[53] Kahlon, S., Beeri, K., Ohkawa, H., Hihara, Y. et al., A putative sensor kinase, Hik31, is involved in the response of *Synechocystis* sp. strain PCC 6803 to the presence of glucose. *Microbiology* 2006, *152*, 647–655.
[54] Huege, J., Goetze, J., Schwarz, D., Bauwe, H. et al., Modulation of the major paths of carbon in photorespiratory mutants of *Synechocystis*. *PLoS One* 2011, *6*, e16278.